recycling

MDPI

Article

Study of the Mechanical and Electrochemical Performance of Structural Concrete Incorporating Recycled Polyethylene Terephthalate as a Partial Fine Aggregate Replacement

Ana Cecilia Espindola-Flores [1,2], Michelle Alejandra Luna-Jimenez [1], Edgar Onofre-Bustamante [1,*] and Ana Beatriz Morales-Cepeda [2]

[1] Instituto Politécnico Nacional-Centro de Investigación en Ciencia Aplicada y Tecnología Avanzada, Unidad Altamira, Km. 14.5 Carretera Tampico-Puerto Industrial Altamira, Altamira 89600, Mexico; aespindolaf@ipn.mx (A.C.E.-F.); mlunaj2000@alumno.ipn.mx (M.A.L.-J.)

[2] Centro de Investigación en Petroquímica, Instituto Tecnológico de Ciudad Madero, Tecnológico Nacional de México, Bahía de Aldhair S/N, Altamira 89600, Mexico; ana.mc@cdmadero.tecnm.mx

* Correspondence: eonofre@ipn.mx

Abstract: The extraction of materials, such as sand and gravel, required for the manufacture of concrete results in the overexploitation of natural resources and a large release of CO_2 emissions into the environment. Therefore, the search for alternatives to partially replace these aggregates has become an important issue to solve. Nonetheless, the demand for producing sustainable yet high-strength and durable concrete using alternative materials has led concrete technologists to develop high-performance concrete. These novel concretes possess superior engineering properties, such as high durability and ductility, low maintenance costs, high mechanical strength, and prolonged service life. Currently, there is significant interest in the development of concrete–polymer compounds, primarily to improve the mechanical properties of the material. In this context, the present study explores the partial replacement of fine aggregate with recycled Polyethylene terephthalate (R-PET) in different proportions to produce green structural concrete, with the aim of studying its impact on the mechanical and electrochemical properties. The mechanical properties evaluated were the compressive and flexural strengths, while the electrochemical properties were evaluated through the open circuit potential and polarization curves. The results indicated that specimens containing different R-PET percentages as a replacement for fine aggregate showed higher increases in compressive and flexural strengths. It was also found that the presence of R-PET decreased the corrosion rate of the reinforcing steel when seawater was used as the electrolyte.

Keywords: concrete; recycled PET; mechanical properties; corrosion

check for updates

Citation: Espindola-Flores, A.C.; Luna-Jimenez, M.A.; Onofre-Bustamante, E.; Morales-Cepeda, A.B. Study of the Mechanical and Electrochemical Performance of Structural Concrete Incorporating Recycled Polyethylene Terephthalate as a Partial Fine Aggregate Replacement. *Recycling* **2024**, *9*, 51. https://doi.org/10.3390/recycling9030051

Academic Editors: Domenico Asprone and Michele John

Received: 12 February 2024
Revised: 14 May 2024
Accepted: 13 June 2024
Published: 20 June 2024

Copyright: © 2024 by the authors. Licensee MDPI, Basel, Switzerland. This article is an open access article distributed under the terms and conditions of the Creative Commons Attribution (CC BY) license (https://creativecommons.org/licenses/by/4.0/).

1. Introduction

The increasing volume of housing and infrastructure construction in many countries around the world highlights the need to sustainably use natural resources. Concrete is the most consumed building material [1], with aggregates (i.e., natural sand, gravel, and crushed stone) constituting 60–80% of its composition [2,3]. In recent years, the building and construction sector has consumed over 40 Gt of aggregates per year [4,5]. According to the projections of Kirthika et al. [6], the demand for raw materials in the construction sector could double by 2030. Overconsumption, flaws in applied technologies for mining operations, and the legal regulations of natural resource extraction activities [7] lead to resource depletion and have negative environmental consequences, including the disturbance of terrestrial landscapes [8], changes in riverbed geometry [9], the disturbance of local flora and fauna [10,11], and the deterioration of both groundwater and surface water quality [10,12].

Additionally, the construction industry is responsible for at least 50% of the current CO_2 pollutant emissions [13,14] because of the overexploitation of materials such as sand and gravel and is considered to be one of the most severely polluting industries according to the National Housing Commission (CONAVI) [15,16]. For these reasons, the search for alternatives for the total or partial replacement of these aggregates has become increasingly imperative.

Considering the current global situation and possible future implications, the United Nations assented to establish actions to protect the planet, which were adopted in 2015: an agenda of global objectives aimed at ending poverty, protecting the planet, and ensuring prosperity for all. In this context, using recycled Polyethylene terephthalate (R-PET) contributes to Sustainable Development Goal No. 11, which emphasizes the development of sustainable cities and communities. To achieve this, it is necessary to transform the way we currently build and explore alternatives, such as green concrete. Another notable Sustainable Development Goal is No. 12: responsible consumption and production. By utilizing R-PET in concrete, we have the opportunity to develop a circular economy model that will encourage the collection and reuse of this type of waste in a more efficient way that benefits sections of the population and generates employment [17]. These actions also contribute to the targets of the United Nations to drastically reduce emissions in the construction industry. With a target set for 2050, the aim is to achieve "net zero emissions in the building and construction sector" [18].

Nonetheless, the demand for producing sustainable yet high-strength and durable concrete utilizing alternative materials has shifted the attention of concrete technologists towards developing high-performance concrete with superior engineering properties, such as high durability and ductility, low maintenance costs, high mechanical strength, and prolonged service life [19–22]. Recently, the use of plastic waste as a construction material for conventional mortar and concrete has been extensively investigated. As a replacement for fine aggregate, one study reported that 10% sand by volume with plastic waste showed satisfactory performance in terms of improving the mechanical properties of concrete. This has the potential to save millions of tons of sand every year [15,16,23]. It was found that the compressive strength of concrete with 15% (by volume) plastic waste aggregate in the replacement of sand was comparable to that of the control concrete, with a value of 18.34 MPa after 28 days of curing. Therefore, the use of plastic waste in concrete for structural applications is promising. Additionally, an increase in the workability values of concrete mixtures containing plastic aggregate (5–10% by weight) was reported, as plastic does not absorb any water during mixing [24–26]. Other research studies have also reported the benefits of using plastic waste as a replacement for coarse aggregate in concrete.

Some factors, including the aggregate-to-cement ratio, the cementitious material content, the water/cement ratio, and the cement paste thickness, are important when producing good-quality concrete. As the interest in utilizing plastic waste for construction grows, research into the impact of incorporating plastic waste, especially recycled PET plastic, to replace fine or coarse aggregate in structural, pervious, or porous concrete is both intriguing and highly promising, particularly concerning environmental considerations [27,28].

The present study investigates the partial replacement of fine aggregate by R-PET waste in different proportions for the manufacture of structural concrete, with the aim of studying its impact on the mechanical and electrochemical properties of the concrete–steel reinforcement system. The mechanical properties were evaluated based on the compressive and flexural strengths, while the electrochemical properties were evaluated using the open circuit potential (OCP) and polarization curves (PCs).

2. Experimental Section

2.1. Characterization of R-PET

Residue-free R-PET was selected and ground using two different types of equipment to obtain a homogeneous material with particle sizes between 0.25 and 0.45 mm, similar to that of fine aggregate (sand), facilitating the integration and homogenization of R-PET into

the concrete matrix. The equipment used to achieve this was a Nelmor blade mill (coarse grinding) Twinsburg, OH, USA, followed by grinding (cutting and shearing) using a Retsch mill model SM2000 (fine grinding), Düsseldorf, Germany.

2.2. X-ray Diffraction

The R-PET samples were analyzed to determine their structure by X-ray diffraction (XRD) using a Bruker D8 Advance diffractometer (Madison Wisconsin, WI, USA) with a 2θ Bragg–Brentano configuration over the range of 5°–90° at a speed of 0.02°/s, with radiation Cu-Kα (λ = 1.5406 Å) operating at a voltage of 40 kV and a current of 40 mA. The samples included R-PET in film form (R-PET-F), the first R-PET grind (R-PET-G1), and the second R-PET grind (R-PET-G2) to determine whether the grinding process produced a structural change in the R-PET.

2.3. Concrete Mixture Design

The design of the concrete mixtures was carried out in accordance with guidelines from the American Concrete Institute (ACI) [29]. The amounts of fine aggregate to be replaced by R-PET were calculated as 2.5, 5, and 10 wt% for the R-PET particles obtained from the second grinding process, denoted as R-PET-G2. This study consisted of two stages. The first stage involved the creation of cylindrical and rectangular specimens, which were hardened for periods of 7, 14, 28, and 180 days. After the curing period, each specimen was mechanically characterized to obtain its compressive and flexural strengths and determine the effect of the addition of R-PET on its mechanical behavior. In the second stage, the effect of adding crushed R-PET to the concrete–steel system was studied by analyzing its electrochemical behavior. The specimens used in the study were rectangular (to simulate a concrete pile with a 1/10 ratio), with each sample containing two reinforcing steel bars (working electrode) and a stainless steel bar (counter electrode) to conduct electrochemical tests.

2.4. Mechanical Characterization

2.4.1. Compressive Strength

The compressive strength test was conducted on 100/200 mm concrete cylinder specimens after water curing for 7, 14, 28, and 180 d. The specimens were dried at room temperature for 24 h before the testing day. The ASTM C39/C39M18 standard test method for testing the compressive strength of cylindrical concrete specimens [30] was used to conduct the compression test. The concrete sample was placed on a universal testing machine (UTM), and a load was applied until fracture. Tests were performed in triplicate, and the results were analyzed to determine the effect of the addition of R-PET. The specimens were identified based on the percentage of added R-PET as follows: a reference specimen (C-R) and specimens with substitutions of 2.5, 5, and 10 wt% (C-P2.5, C-P5, and C-P10, respectively).

2.4.2. Flexural Strength

Rectangular specimens with dimensions of 150 × 150 × 600–750 mm were used to determine the flexural strength using a UTM in accordance with ASTM C293/293M (center load method) [31]. Tests were performed in triplicate to determine the effect of the addition of R-PET on the mechanical properties of the concrete. The specimens were evaluated under the same conditions (water curing for 7, 14, 28, and 180 days) and identified in the same manner as the compression test samples.

2.5. Electrochemical Characterization

For the electrochemical tests, a specimen was designed based on the arrangement of three electrodes: a working electrode (3/8″ reinforcing steel), an auxiliary electrode (stainless steel), and a reference electrode (saturated calomel), as displayed in Figure 1. The specimens were exposed to seawater to simulate an aggressive medium for concrete, and

the effect of the addition of R-PET on the electrochemical behavior of the concrete samples (corrosion rate) was determined. The samples were characterized using electrochemical techniques. OCP was applied for over 20 min to allow for stabilization of the system before polarizing. Tafel curves were created by applying a polarization potential of ±300 mV with respect to the corrosion potential, with a sweep speed of 0.5 mV/s, to explore the corrosion current density and the corrosion rate.

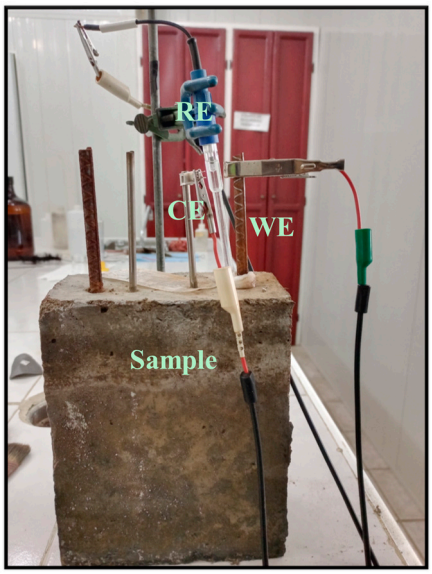


Figure 1. Experimental design for electrochemical evaluation.

3. Results and Analysis

3.1. Characterization of R-PET by X-ray Diffraction

The different R-PET samples were characterized, including the film sample (R-PET-F) and the crushed and ground R-PET samples (R-PET-G1, G2). The crystallinity parameters for R-PET were reported as a triclinic structure with lattice parameters of α = 0.444 nm, b = 0.591 nm, c = 1.067 nm, $\alpha = 100°$, $\beta = 117°$, $\Upsilon = 112°$, V = 0.210 nm^3, and d = 1.52 g/cm^3 [32], as provided in Table 1.

Table 1. PET Miller indices [33].

Miller Index	2θ Location
011	16.43
010	17.54
111	21.56
110	22.85
103	25.28
100	26.12
111	27.77–28.46
101	32.51

In Figure 2, the main diffraction peak is observed at the maximum point of 2θ = 26° in the (100) plane, which is characteristic of a semicrystalline PET structure, as reported in the literature [34]. The diffractogram for the R-PET-G2 sample shows a decrease in the signal intensity and a lower definition compared to R-PET-F. This is a result of the irregularity and morphology of the sample—grinding roughened the surface of the R-PET particles, preventing the crystals from being correctly oriented. Therefore, because the X-ray beam

does not find a surface oriented in a single direction, the strength of the corresponding signals decreases. The sample in film form (R-PET-F) had R-PET particles that were oriented homogeneously over a short distance, generating a greater intensity in the XRD signal.

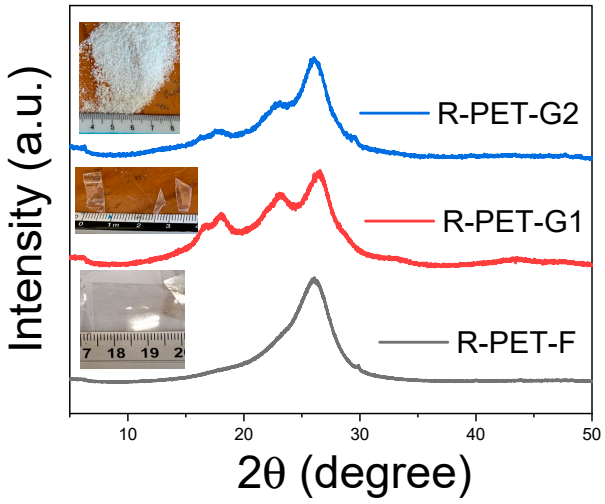


Figure 2. Diffractograms obtained from the different samples of the film and ground R-PET-F, R-PET-G1, and R-PET-G2.

3.2. Tests of Concrete Specimens

From the mixture design, we obtained the aggregate dosage, as shown in Table 2. f'c = 40 MPa, and the water-to-cement ratio (w/c) ratio was 0.45.

Table 2. Mixtures design.

Sample	Mixture Component kg/m^3				
	Cement	**Water**	**Coarse**	**Fine**	**R-PET**
C-R	395	180	952.8	861.3	0
C-P2.5	395	180	952.8	839.76	21.53
C-P5	395	180	952.8	818.23	43.06
C-P10	395	180	952.8	775.17	86.13

Figure 3 shows the C-P5 specimens obtained using the aggregate dosage displayed in Table 2 before mechanical characterization.



Figure 3. Test specimens of C-P5 obtained after 28 days of curing.

3.2.1. Mechanical Characterization

The results of the compression tests were obtained based on the four curing periods of 7, 14, 28, and 180 days (Table 3). The results showed that for the modified specimens cured for 7, 14, and 28 days, increasing the R-PET content reduced the compressive strength. The C-P10 mixture had the lowest values of compressive strength (34.2 and 45.8 MPa at 7 and 28 days, respectively). This behavior arises from the presence of R-PET in the concrete mixture. R-PET causes a decrease in the cement hydration rate or alkali-hydrolysis reaction, thus preventing water from reacting with the main compounds in cement, such as tricalcium silicate, dicalcium silicate, tricalcium aluminate, and tetracalcium ferroaluminate (tetracalcium aluminum ferrite) [35,36]. This slows down the hardening of the mixture, meaning that it takes longer to completely harden and reach the maximum resistance. Furthermore, the hydrophobic nature of R-PET delays cement hydration [37,38] by restricting the movement of water, which is useful in terms of enabling the alkali-hydrolysis reaction (cement hydration) to form a hardened matrix. Hence, curing for over 28 days does not allow the peak mechanical properties and characteristics of this type of concrete to be achieved [39]. However, all the samples modified with R-PET (C-P2.5, C-P5, and C-P10) cured for 28 days showed a mechanical strength that was higher than the expected value (40 MPa) for this type of concrete. After curing for 180 days, the reference specimen (C-R) did not show a significant change in compressive strength compared to the value after curing for 28 days, whereas the samples modified with R-PET showed a significant increase in their compressive strength. This behavior can be attributed to the presence of R-PET, primarily because of the sufficient time elapsed for cement hydration, allowing alkali-hydrolysis reactions to occur. As R-PET absorbs water, its potential for water accumulation is diminished [40,41].

Table 3. Compressive strength test results (MPa).

Sample	Curing Days			
	7	**14**	**28**	**180**
C-R	49.4	55.4	59.8	60.8
C-P2.5	43	52	54.9	62.1
C-P5	38.4	51.5	60.2	72.0
C-P10	34.2	38.6	45.8	56.9

Therefore, a mature, hardened matrix is formed with mechanical properties that are superior to those of the reference sample. Additionally, R-PET absorbs part of the energy applied during the compression test, taking advantage of PET's main mechanical characteristics, such as its high compressive and tensile strengths (40 MPa), Young's modulus of 1700 MPa, and impact resistance of 90 J/m. However, sample C-P5 had the highest compressive strength value of 72 MPa, approximately 20% higher than that of the value for the C-R sample and about 80% higher than that of the estimated value (40 MPa). These results can be seen in Figure 4. It is important to note that the quality of concrete depends on the quality of the paste, aggregates, and the bond between them. In properly made concrete, every aggregate particle is completely covered by cementitious paste, and all the spaces between these particles are filled with the paste. The presence of R-PET may reduce the wettability of the aggregates and cementitious paste.

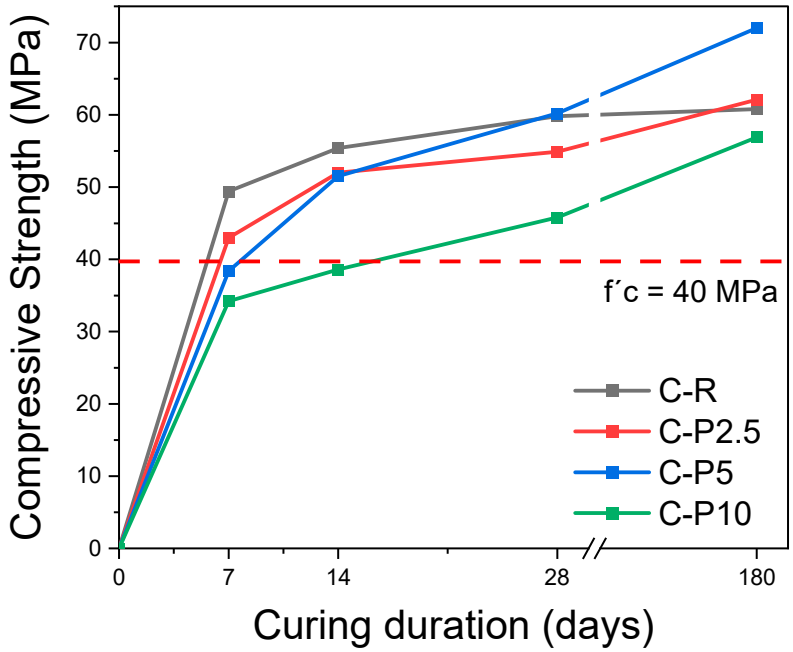


Figure 4. Evolution of the compressive strength of the different specimens at 7, 14, 28, and 180 curing days.

3.2.2. Flexural Strength

The results of the flexural strength tests were obtained over the same time periods as the compressive strength tests, i.e., 7, 14, 28, and 180 curing days, and are shown in Table 4.

Table 4. Rupture modulus results (MPa).

Samples	Curing Days			
	7	**14**	**28**	**180**
C-R	3.5	4.4	4.5	4.6
C-P2.5	3.1	4.0	4.3	5.6
C-P5	3.6	4.0	4.4	5.8
C-P10	3.5	4.1	5.0	5.4

Similar results are observed for the modified samples and the reference sample after 7, 14, and 28 days of curing. The C-P10 sample has the best mechanical performance. However, after 180 days of curing, the modified samples show a significant increase in flexural strength, reaching values close to 6 MPa, i.e., at least 30% higher than that of the reference sample, which had a maximum flexural strength of 4.6 MPa, and 41.5% higher than the estimated value for this type of concrete (4.1 MPa). These results can be seen in Figure 5. This behavior is associated with the presence of R-PET in the concrete mixture, which decreases the cement hydration rate, thus inhibiting the alkali-hydrolysis reactions. This slows down the hardening of the mixture, meaning that it takes longer to completely harden and reach its maximum resistance. This finding is consistent with the results obtained for the compressive strength. When the curing period is 180 days, enough time has passed to allow the cement to hydrate, i.e., the alkali-hydrolysis reactions proceed and the R-PET absorbs water, favoring the formation of a mature, hardened matrix with better mechanical properties than the reference sample. In addition, the presence of R-PET allows the concrete to absorb part of the energy applied during the flexural strength test [40,41].

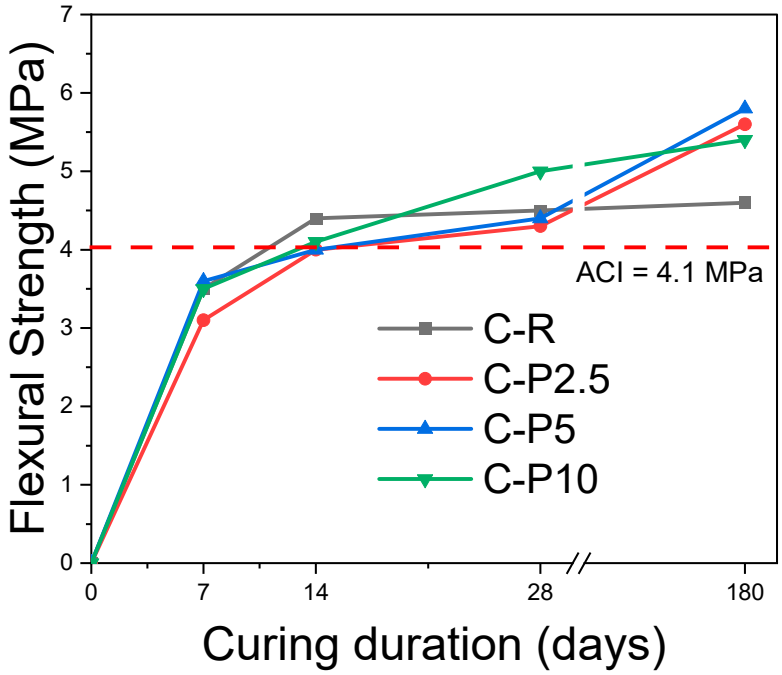


Figure 5. Evolution of the flexural strength of the different specimens after 7, 14, 28, and 180 days of curing.

3.2.3. Electrochemical Characterization

Open-Circuit Potential (OCP)

The corrosion potential of the reinforcing steel (rod) in different specimens modified with R-PET and the reference specimen was monitored based on the OCP as a function of time. To carry out this measurement, the modified and unmodified concrete samples were exposed to seawater for 6 and 12 months to determine the effect of R-PET on the electrochemical properties of the reinforced concrete–steel system.

Table 5 shows that for most of the specimens, after exposure to seawater for 6 months, the potential of the reinforcing steel shifts towards more positive values of around 150 mV with respect to the bare steel potential.

Table 5. OCP results of the specimens exposed to seawater for 6 and 12 months.

Sample	6 Months E (mV)	12 Months E (mV)
C-R	−433.2	−325.3
C-P2.5	−304.7	−439.58
C-P5	−271.2	−546.65
C-P10	−248.8	−486.08

Taking the iron potential (reinforcing steel) as a reference, which is close to −0.44 V vs. the NHE (normal hydrogen electrode) or equivalent to −0.520 V vs. the SCE (saturated calomel electrode), the initial value for the reference sample shows a value typical of an active surface. Under the pH conditions characteristic of fresh concrete, this surface can undergo passivation, generating iron oxy-hydroxide mixtures like goethite (α-FeOOH), lepidocrocite (γ-FeOOH), and akaganeite (β-FeOOH). These compounds, which are reported as the first iron-based, semi-stable species, facilitate the passivation of the reinforcing steel under specific potential and pH conditions [42]. It can also be observed that the presence of R-PET in the modified specimens shifts the potential to more positive (nobler) values (Figure 6). This could be because R-PET has properties that allow it to act as a barrier

against aggressive ions and gases, such as Cl^-, O_2, and CO_2. Therefore, it may inhibit the access of these aggressive species, keeping the passive film stable.

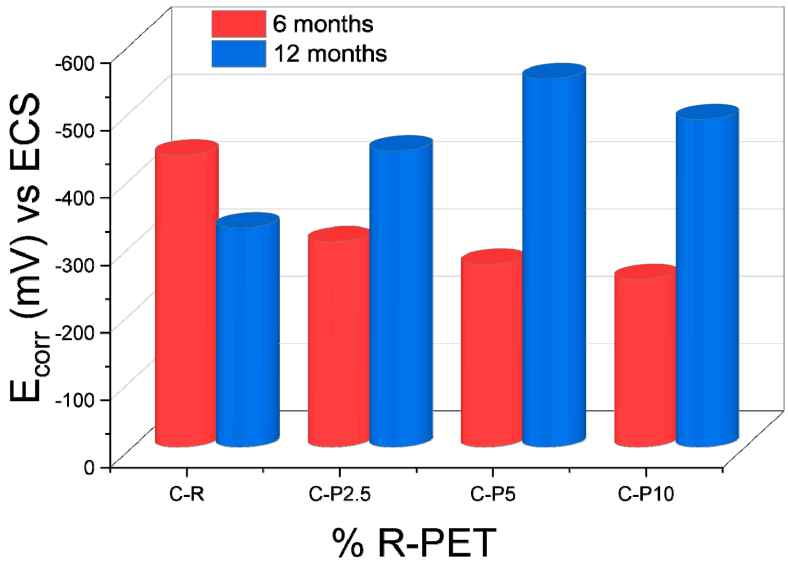


Figure 6. OCP behavior of the specimens exposed to seawater for 6 and 12 months.

From the potentials obtained after 12 months of seawater exposure, the opposite behavior is observed compared to the first 6 months of evaluation, with a shift towards more negative (or active) values of at least 100 mV. A maximum displacement of 221 mV in the negative direction is reached for the C-P5 sample with respect to the C-R sample. From a thermodynamic perspective, this behavior may be associated with the rupture of the passive film that formed on the reinforcing steel because of water ingress. This allows aggressive ions (mainly Cl^- and O_2) to penetrate the concrete matrix until the surface of the reinforcing steel is reached, thus breaking the passive film, activating the surface, and initiating oxide-reduction reactions.

3.2.4. Tafel Extrapolation

The Tafel extrapolation curves obtained from specimens exposed to seawater for 6 months revealed a notable shift toward more positive corrosion potential values and slightly lower corrosion current densities (i_{corr}). This observed behavior aligns with the earlier discussion regarding E_{corr}, where it was proposed that this displacement was associated with the presence of R-PET. By acting as a barrier, R-PET prevents the ingress of water and aggressive ions, such as Cl^-, O_2, and CO_2, which keeps the passive film stable and free from pitting corrosion.

These samples show a lower V_{corr} than the C-R sample, as shown in Table 6. However, after 12 months of exposure to seawater, the specimens modified with R-PET showed the opposite behavior to that observed after 6 months of exposure, as the polarization curves for the samples modified with R-PET underwent a potential shift to more active (negative) values compared to the C-R sample.

This behavior could be explained by the fact that after 12 months of exposure to water, aggressive ions (such as Cl^-), O_2, and CO_2, could have entered and penetrated the concrete matrix to reach the surface of the reinforcing steel. This would break the passive film and activate the surface, initiating oxide-reduction reactions. However, the samples modified with R-PET, despite showing a more active E_{corr}, have lower corrosion current densities (i_{corr}) than the C-R sample, as can be seen in Figure 7. This may be related to the surface activation, as E_{corr} is more active. During the establishment of oxide-reduction reactions, the oxidation of the reinforcing steel is temporarily favored, effectively masking the damage to the passive film that naturally forms on the reinforcing steel surface, leading to a lower

value of i_{corr}. However, depending on the exposure period and as a result of the formation of bulkier oxides, there will be higher rates of corrosion and even cracks in the concrete, as reported in the literature [43,44].

Table 6. Electrochemical parameters of the specimens evaluated in seawater.

Specimen	Potential (mV)	i_{corr} mA/cm^2	V_{corr} mmy	V_{corr} mpy
6-month evaluation				
C-R	−552	1.28×10^{-2}	0.1483	5.8400
C-P2.5	−413	3.89×10^{-3}	0.0450	1.7748
C-P5	−398	3.31×10^{-3}	0.0383	1.5101
C-P10	−382	8.91×10^{-4}	0.0103	0.4065
12-month evaluation				
C-R	−348	3.98×10^{-3}	0.0461	1.8158
C-P2.5	−506	1.9×10^{-3}	0.0220	0.8668
C-P5	−615	7.58×10^{-3}	0.0087	0.3458
C-P10	−389	1.04×10^{-3}	0.0120	0.4745

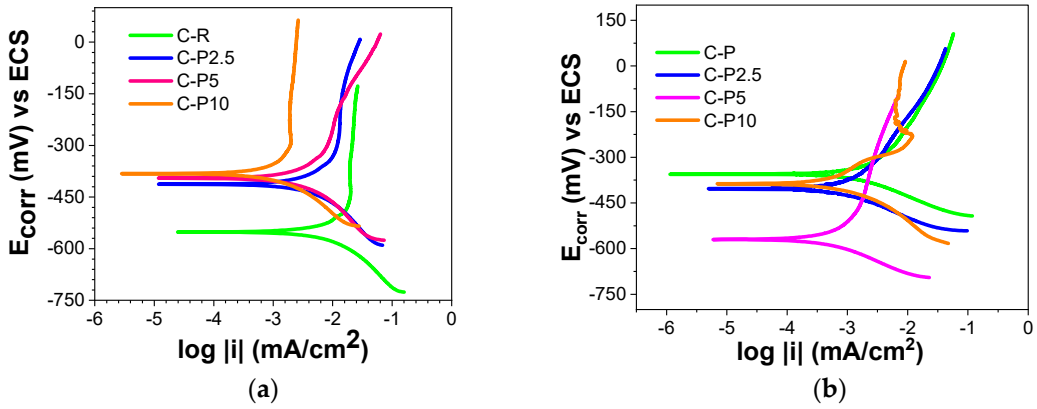


Figure 7. Tafel extrapolation results of the specimens after (**a**) 6 and (**b**) 12 months of seawater exposure.

4. Conclusions

In this work, we proposed the partial replacement of fine aggregate with recycled PET in structural concrete and determined the corresponding effects on its mechanical and electrochemical properties. The following conclusions were drawn:

It was determined that the addition of R-PET particles with a homogenous particle size close to that of the fine aggregate (≈0.35 mm) strongly increased the compressive and flexural strengths.

Sample C-P5 showed a compressive strength higher (by approximately 20%) than that of the value for the reference sample (C-R), while it was about 80% higher than the expected value (40 MPa). In the same sample, the flexural strength was 30% higher than that of C-R (4.6 MPa) and 41.5% higher than the estimated value for this type of concrete (4.1 MPa).

Additionally, it was found that the presence of R-PET in the concrete mixture decreased the cement hydration and the alkali-hydrolysis reaction rate. This was a result of the hydrophobic nature of PET, which inhibited water from reacting with the main cement compounds and slowed down the hardening of the mixture.

From the electrochemical evaluation, it was determined that the addition of R-PET shifted the potential towards more positive values as a function of time. This prevented the

ingress of aggressive ions like Cl^-, as well as O_2 and CO_2, thus maintaining the stability of the passive film (iron oxide-hydroxides). Consequently, the reinforcing steel remained protected without any signs of pitting corrosion.

Finally, these results confirm that the utilization of R-PET is a promising route to produce green concrete with excellent mechanical and electrochemical properties for application in the construction industry. This will reduce extraction costs and the use of non-renewable natural resources, contributing to a reduction in the carbon footprint associated with the construction industry.

Author Contributions: A.C.E.-F.: experimental methodology and the data cu-ration, founding acquisition and writing–review and editing; M.A.L.-J.: experimental methodology. E.O.-B.: investigation, resources, writing-review and editing and project administration. A.B.M.-C.: writing-review and editing. All authors have read and agreed to the published version of the manuscript.

Funding: This research has been carried out with the support of the Instituto Politécnico Nacional under the SIP-20231307 and SIP-20230611 projects.

Data Availability Statement: The data presented in this study are available on request from the corresponding author.

Acknowledgments: We appreciate the collaboration of the company Concretos Tancol S.A. de C.V., under the supervision of Eng. José Antonio Cristóbal Hernández, for the development of the concrete mixtures.

Conflicts of Interest: The authors declare no conflict of interest.

References

1. Gagg, C.R. Cement and concrete as an engineering material: An historic appraisal and case study analysis. *Eng. Fail. Anal.* **2014**, *40*, 114–140. [CrossRef]
2. Mo, K.H.; Thomas, B.S.; Yap, S.P.; Abutaha, F.; Tan, C.G. Viability of agricultural wastes as substitute of natural aggregate in concrete: A review on the durability related properties. *J. Clean. Prod.* **2020**, *275*, 123062. [CrossRef]
3. Alqahtani, F.K.; Zafar, I. Plastic-based sustainable synthetic aggregate in Green Lightweight concrete—A review. *Construct. Build. Mater.* **2021**, *292*, 123321. [CrossRef]
4. Yehia, S.; Helal, K.; Abusharkh, A.; Zaher, A.; Istaitiyeh, H. Strength Durability Evaluation of Recycled Aggregate Concrete. *Int. J. Concrete Struct. Mater.* **2015**, *9*, 219–239. [CrossRef]
5. Ren, Z.; Jiang, M.; Chen, D.; Yu, Y.; Li, F.; Xu, M.; Bringezu, S.; Zhu, B. Stocks and flows of sand, gravel, and crushed stone in China (1978–2018): Evidence of the peaking and structural transformation of supply and demand. *Resour. Conserv. Recycl.* **2022**, *180*, 106173. [CrossRef]
6. Kirthika, S.K.; Singh, S.K.; Chourasia, A. Alternative fine aggregates in production of sustainable concrete—A review. *J. Clean. Prod.* **2020**, *268*, 122089. [CrossRef]
7. Gavriletea, M.D. Environmental impacts of sand exploitation. Analysis of sand market. *Sustainability* **2017**, *9*, 1118. [CrossRef]
8. Timofeeva, Y.R.; Suhacheva, E.Y.; Zakharova, M.K. Soil cover of areas of mining sand and sand-gravel material in the Leningrad region. *IOP Conf. Ser. Earth Environ. Sci.* **2021**, *862*, 012064. [CrossRef]
9. Meador, M.R.; Layher, A.O. Instream sand and gravel mining: Environmental issues and regulatory process in the United States. *Fisheries* **1998**, *23*, 6–13.
10. Bayram, A.; Onsoy, H. Sand and gravel mining impact on the surface water quality: A case study from the city of Tirebolu (Giresun Province, NE Turkey). *Environ. Earth Sci.* **2015**, *73*, 1997–2011. [CrossRef]
11. Padmalal, D.; Maya, K.; Sreebha, S.; Sreeja, R. Environmental effects of river sand mining: A case from the river catchments of Vembanad lake, Southwest coast of India. *Environ. Geol.* **2008**, *54*, 879–889. [CrossRef]
12. Yen, T.P.; Rohasliney, H. Status of water quality subject to sand mining in the Kelantan River, Kelantan. *Trop. Life Sci. Res.* **2013**, *24*, 19–34.
13. Leonhardt, F. *Estructuras de Hormigón Armado*, 3rd ed.; El Ateneo: Madrid, Spain, 1986.
14. Ruiz, J.L.R.; Hernández, C.G.C.; López, R.C.; Hernández, R.N. Diseño de un sistema autoconstructivo a base de tapial y bahareque de bajo costo e impacto ambiental para una vivienda. *Tópicos Investig. Cienc. Tierra Mater.* **2020**, *7*, 68–78. [CrossRef]
15. Kore, S.D. Sustainable Utilization of Plastic Waste in Concrete Mixes—A Review. *J. Build. Mater. Struct.* **2019**, *5*, 212–217. [CrossRef]
16. Thorneycroft, J.; Orr, J.; Savoikar, P.; Ball, R.J. Performance of structural concrete with recycled plastic waste as a partial replacement for sand. *Constr. Build. Mater* **2017**, *161*, 63–69. [CrossRef]
17. Naciones Unidas. Available online: https://www.un.org/sustainabledevelopment/es/objetivos-de-desarrollo-sostenible/# (accessed on 19 March 2024).

18. Naciones Unidad México. Available online: https://mexico.un.org/es/245562-plan-de-las-naciones-unidas-promete-enormes-reducciones-de-emisiones-en-el-sector-de-la (accessed on 20 March 2024).
19. Shi, Y.; Long, G.; Zen, X.; Xie, Y.; Shang, T. Design of binder system of eco-efficient UHPC based on physical packing and chemical effect optimization. *Constr. Build. Mater.* **2020**, *274*, 121382. [CrossRef]
20. Gu, C.; Ye, G.; Sun, W. Ultrahigh performance concrete-properties, applications and perspectives. *Sci. China Technol. Sci.* **2015**, *58*, 587–599. [CrossRef]
21. Zeyad, A.M.; Hakeem, I.Y.; Amin, M.; Tayeh, B.A.; Agwa, I.S. Effect of aggregate and fibre types on ultra-high-performance concrete designed for radiation shielding. *J. Build. Eng.* **2022**, *58*, 104960. [CrossRef]
22. Amin, M.; Hakeem, I.Y.; Zeyad, A.M.; Tayeh, B.A.; Maglad, A.M.; Agwa, I.S. Influence of recycled aggregates and carbon nanofibres on properties of ultra-high- performance concrete under elevated temperatures. *Case Stud. Constr. Mater.* **2022**, *16*, e01063. [CrossRef]
23. Jambeck, J.R.; Geyer, R.; Wilcox, C.; Siegler, T.R.; Perryman, M.; Andrady, A.; Narayan, R.; Law, K.L. Plastic waste inputs from land into the ocean. *Science* **2015**, *347*, 768–771. [CrossRef]
24. Subrmani, T.; Pugal, V.K. Experimental study on plastic waste as a coarse aggregate for structural concrete. *Int. J. Appl. Innov. Eng. Manag.* **2015**, *4*, 144–152.
25. Habib, M.Z.; Alom, M.M.; Hoque, M.M. Concrete production using recycled waste plastic as aggregate. *J. Civ. Eng.* **2017**, *45*, 11–17.
26. Patil, B.; Agrawal, P.S.D. An experimental study on partial replacement of coarse aggregate by using recycled plastic aggregate on strength of concrete. *Int. J. Eng. Technol. Res.* **2018**, *8*, 2454–4698.
27. Manjunath, B.T.A. Partial replacement of E-plastic Waste as Coarse-aggregate in Concrete. *Procedia Environ. Sci.* **2016**, *35*, 731–739. [CrossRef]
28. Jaivignesh, B.; Sofi, A. Study on mechanical properties of concrete using plastic waste as an aggregate. *IOP Conf. Ser. Earth Environ. Sci.* **2017**, *80*, 012016. [CrossRef]
29. *ASTM C33/C33M-18*; Standard Specification for Concrete Aggregates. ASTM: West Conshohocken, PA, USA, 2018.
30. *ASTM C39/C39M-18*; Standard Test Method for Compressive Strength of Cylindrical Concrete Specimens. ASTM International: West Conshohocken, PA, USA, 2018.
31. *ASTM-C-293-02*; Standard Test Method for Strength of Concrete (Using Simple Beam with Center Point Loading). ASTM International: West Conshohocken, PA, USA, 2004.
32. Kirk-Othmer. *Enciclopedia of Chemical Technology*, 3rd ed.; Wiley: New York, NY, USA, 1978.
33. Esparza-Juárez, M.E. Evaluación del Efecto de Parámetros de Proceso Sobre las Propiedades de Piezas de PET y PBT Moldeadas por Inyección. Master's Thesis, Centro de Investigación en Química Aplicada, Saltillo, Mexico, 2005.
34. Jiří, H.; Petr, S.; Petr, S. Volume relaxation in amorphous and semicrystalline PET. *J. Mater. Sci.* **2007**, *42*, 3724–3731. [CrossRef]
35. Rajabipour, F.; Giannini, E.; Dunant, C.; Ideker, J.H.; Thomas, M.D. Alkali-Silica reaction: Current understanding of the reaction mechanisms and the knowledge gaps. *Cem. Concr. Res.* **2015**, *76*, 130–146. [CrossRef]
36. Thomas, M. The effect of supplementary cementing materials on alkali-silica reaction: A review. *Cem. Concr. Res.* **2011**, *41*, 1224–1231. [CrossRef]
37. Calavera, J. *Manual de Ferralla*, 3rd ed.; Intemac: Torrejón de Ardoz, Spain, 2003; Chapter 2.
38. Meseguer, A.G. *Hormigón Armado*, 15th ed.; Gustavo Gili: Barcelona, Spain, 2010.
39. Russo, C. *Obras Hormigón Armado*, 1st ed.; Gustavo Gili: Barcelona, Spain, 1942.
40. Ismail, Z.Z.; AL-Hashmi, E.A. Use of waste plastic in concrete mixture as aggregate replacement. *Waste Manag.* **2008**, *28*, 2041–2047. [CrossRef]
41. Rai, B.; Rushad, S.T.; Kr, B.; Duggal, S.K. Study of waste plastic mix concrete with plasticizer. *ISRN Civil. Eng.* **2012**, *2012*, 469272. [CrossRef]
42. Mejía, C.E.; Vásquez, C.; Peña, D.Y.; Estupiñán, H. Determinación de la despasivación en varillas de acero de refuerzo en solución poro de agua de mar por medio de técnicas electroquímicas. *Prospectiva* **2011**, *9*, 13–20.
43. Castellote, M.; Andrade, C.; Alonso, C. Accelerated simultaneous determination of the chloride depassivation threshold and of the nonstationary diffusion coefficient values. *Corros. Sci.* **2002**, *44*, 2409–2424. [CrossRef]
44. Alonso, C.; Castellote, M.; Andrade, C. Chloride threshold dependence of pitting potential of reinforcements. *Electrochim. Acta* **2002**, *47*, 3469–3481. [CrossRef]

Disclaimer/Publisher's Note: The statements, opinions and data contained in all publications are solely those of the individual author(s) and contributor(s) and not of MDPI and/or the editor(s). MDPI and/or the editor(s) disclaim responsibility for any injury to people or property resulting from any ideas, methods, instructions or products referred to in the content.